

Sterol carrier protein-2 (SCP-2) involvement in cholesterol hydroperoxide cytotoxicity as revealed by SCP-2 inhibitor effects

Tamas Kriska, Anna Pilat, Jared C. Schmitt, and Albert W. Girotti¹

Department of Biochemistry, Medical College of Wisconsin, Milwaukee, WI

Abstract Sterol carrier protein-2 (SCP-2) plays an important role in cholesterol trafficking and metabolism in mammalian cells. The purpose of this study was to determine whether SCP-2, under oxidative stress conditions, might also traffic hydroperoxides of cholesterol, thereby disseminating their cytotoxic effects. Two inhibitors, SCPI-1 and SCPI-3, known to block cholesterol binding by an insect SCP-2, were used to investigate this. A mouse fibroblast transfectant clone (SC2F) overexpressing SCP-2 was found to be substantially more sensitive to apoptotic killing induced by liposomal 7 α -hydroperoxycholesterol (7 α -OOH) than a wild-type control. 7 α -OOH uptake by SC2F cells and resulting apoptosis were both inhibited by SCPI-1 or SCPI-3 at a subtoxic concentration. Preceding cell death, reactive oxidant accumulation and loss of mitochondrial membrane potential were also strongly inhibited. Similar SCPI protection against 7 α -OOH was observed with two other types of SCP-2-expressing mammalian cells. In striking contrast, neither inhibitor had any effect on H₂O₂-induced cell killing. To learn whether 7 α -OOH cytotoxicity is due to uptake/transport by SCP-2, we used a fluorescence-based competitive binding assay involving recombinant SCP-2, NBD-cholesterol, and SCPI-1/SCPI-3 or 7 α -OOH. The results clearly showed that 7 α -OOH binds to SCP-2 in SCPI-inhibitable fashion. Our findings suggest that cellular SCP-2 not only binds and translocates cholesterol but also cholesterol hydroperoxides, thus expanding their redox toxicity and signaling ranges under oxidative stress conditions.—Kriska, T., A. Pilat, J. C. Schmitt, and A. W. Girotti. Sterol carrier protein-2 (SCP-2) involvement in cholesterol hydroperoxide cytotoxicity as revealed by SCP-2 inhibitor effects. *J. Lipid Res.* 2010. 51: 3174–3184.

Supplementary key words oxidative stress • lipid peroxidation • lipid peroxide translocation

This work was supported by National Institutes of Health Grants CA-72630 and HL-85677. Its contents are solely the responsibility of the authors and do not necessarily represent the official views of the National Institutes of Health.

Manuscript received 10 May 2010 and in revised form 23 July 2010.

Published, JLR Papers in Press, July 23, 2010

DOI 10.1194/jlr.M008342

Translocation of nonesterified cholesterol (Ch) from one membrane compartment to another in eukaryotic cells is required for metabolic processing of the sterol and for membrane biogenesis and refashioning (1–3). Spontaneous intermembrane transfer of phospholipids also occurs but generally more slowly than Ch transfer (1, 2). Various Ch transfer proteins exist that can greatly accelerate the desorption of this lipid from a donor membrane and movement to an acceptor. Included among these are the StAR family transfer proteins (4, 5) and sterol carrier protein-2 (SCP-2) (6–8). Unlike the StAR proteins, SCP-2 has broad specificity, facilitating the movement of various phospholipids and fatty acids in addition to Ch (7–9), which explains why it is also referred to as a nonspecific lipid transfer protein. Mature SCP-2 is a relatively small (13.2 kDa) translation product of a fusion gene encoded for 58 kDa SCP-x (most of which is peroxisomal 3-ketoacyl-CoA thiolase) and 15 kDa pro-SCP-2 (7, 8). Immunodetection methods have revealed that the bulk of SCP-2 in most mammalian cells is located in peroxisomes, but significant amounts are also found in mitochondria, lysosomes, and cytosol, probably reflecting its broad-scale lipid trafficking activity (7). In mouse L-fibroblasts, for example, at least 50% of the protein's immunoreactivity is extraperoxisomal (10). One proposed mechanism of SCP-2-facilitated trans-

Abbreviations: 7 α -OOH, 3 β -hydroxycholest-5-ene-7 α -hydroperoxide; Ch, cholesterol; ChOOH, cholesterol hydroperoxide; DCFH-DA, 2',7'-dichlorofluorescein diacetate; DCF, 2',7'-dichlorofluorescein; DCFH-DA, 2',7'-dichlorofluorescein diacetate; DCP, dicycylphosphate; DFO, desferrioxamine; DMPC, 1,2-dimyristoyl-*sn*-glycero-3-phosphocholine; Ho, Hoechst 33258; JC-1, 5,5',6,6'-tetrachloro-1,1',3,3'-tetraethyl-benzimidazolylcarbocyanine iodide; LOOH, lipid hydroperoxide; MTT, 3-(4,5-dimethylthiazolyl-2-yl)-2,5-diphenyltetrazolium bromide; NBD-Ch, 22-[N-(7-nitrobenz-2-oxa-1,3-diazol-4-yl)amino]-23,24-bisnor-5-cholen-3 β -ol; PBS, Chelex-treated phosphate buffered saline (25 mM sodium phosphate, 125 mM NaCl, pH 7.4); PI, propidium iodide; POPC, 1-palmitoyl-2-oleoyl-*sn*-glycero-3-phosphocholine; SCP-2, sterol carrier protein-2; SCPI-1, N-(4-[[4-(3,4-dichlorophenyl)-1,3-thiazol-2-yl]amino]phenyl)acetamide; SCPI-3, 3-(4-bromophenyl)-5-methoxy-7-nitro-4H-1,2,4-benzoxadiazine; SUV, small unilamellar vesicle; ROS, reactive oxygen species; VC, vector control.

¹To whom correspondence should be addressed.

e-mail: agirotti@mcw.edu

fer involves interaction of its cationic N-terminal domain with a donor membrane's anionic surface, binding of an available lipid, and migration to the acceptor membrane for unloading (7, 11). There is also evidence that SCP-2 can bind some lipids in the aqueous compartment following desorption (i.e., without making contact with the donor membrane) (12).

Unsaturated phospholipids and Ch in cell membranes may be degraded via free radical-mediated lipid peroxidation under oxidative stress conditions. Lipid hydroperoxides (LOOH) are prominent intermediates of lipid peroxidation which can contribute to this process by undergoing iron-catalyzed one-electron reduction to free radical species (13, 14). Prior studies with model systems revealed that in addition to undergoing damaging reductive turnover in a membrane of origin, LOOH can desorb and translocate to other membranes, where this process may ensue (15, 16). For Ch-derived hydroperoxides (ChOOH) such as singlet oxygen-generated 5α -OOH and free radical-generated $7\alpha/\beta$ -OOH, the rate of spontaneous intermembrane translocation was found to be substantially greater than that of Ch itself (17). Subsequent work showed that ChOOH transfer could be further accelerated by human recombinant SCP-2, and when isolated mitochondria were used as acceptors, this exacerbated peroxide-induced damage/dysfunction as reflected by loss of membrane potential (18). This was the first reported example of enhanced oxidative toxicity due to LOOH shuttling by a lipid-trafficking protein. In a more recent follow-up to these noncellular studies, we showed that an SCP-2-overexpressing transfectant clone of rat hepatoma cells was much more sensitive to apoptotic killing by liposomal 7α -OOH than a vector control, the evidence linking this to faster peroxide internalization and delivery to mitochondria by the overexpressing cells (19). Although these and related findings were consistent with direct SCP-2 involvement in these effects, substantive supporting evidence was lacking (19). Using two recently discovered hydrophobic inhibitors of mosquito SCP-2 that are close to Ch in molecular mass and bind competitively with it to the protein (20, 21), we now provide such evidence for three different SCP-2-expressing mammalian cell lines exposed to a 7α -OOH challenge.

MATERIALS AND METHODS

General materials

Cholesterol, Chelex-100, desferrioxamine (DFO), H_2O_2 , Hoechst 33258 (Ho), propidium iodide (PI), 5,5',6,6'-tetrachloro-1,1',3,3'-tetraethyl-benzimidazolylcarbocyanine iodide (JC-1), 3-(4,5-dimethylthiazolyl-2-yl)-2,5-diphenyltetrazolium bromide (MTT), Dulbecco's modified Eagle's medium (DMEM), phenol red-free DMEM, fetal bovine serum, and other cell culture materials were from Sigma (St. Louis, MO). $[4-^{14}C]$ Ch (~ 55 mCi/mmol) was obtained from Amersham Biosciences (Arlington Heights, IL). Avanti Polar Lipids (Alabaster, AL) supplied the 1,2-dimyristoyl-*sn*-glycero-3-phosphocholine (DMPC) and 1-palmitoyl-2-oleoyl-*sn*-glycero-3-phosphocholine (POPC). Molecular Probes (Eugene, OR) supplied the 22-[*N*-(7-nitrobenz-2-oxa-1,3-

diazol-4-yl)amino]23,24-bisnor-5-cholesterol-3 β -ol (NBD-Ch; Fig. 1) and 2',7'-dichlorofluorescein diacetate (DCFH-DA). Human recombinant SCP-2 was expressed and isolated as described previously (18). Peroxidase-conjugated anti-rabbit IgG was from MP Biochemicals (Aurora, OH). The SCP-2 inhibitors, *N*-(4-[[4-(3,4-dichlorophenyl)-1,3-thiazol-2-yl]amino]phenyl)acetamidehydrobromide (SCPI-1) and 3-(4-bromophenyl)-5-methoxy-7-nitro-4H-1,2,4-benzoxadiazine (SCPI-3) (structures shown in Fig. 1), were obtained from the Hit2Lead Chemical Store (ChemBridge Corp., San Diego, CA).

Preparation of 7α -OOH and $[^{14}C]7\alpha$ -OOH

3β -Hydroxycholesterol-5-ene- $7\alpha/\beta$ -hydroperoxide (7α -OOH; Fig. 1) was prepared by aluminum phthalocyaninedisulfonate-sensitized photoperoxidation of Ch, as described previously (22). 7α -OOH was separated in two chromatographic steps: (i) reversed-phase HPLC using a C_{18} column (250 \times 4.6 mm; 5 μ m particles) with methanol/isopropanol/acetonitrile/water (70:12:11:7 by vol) as the mobile phase; and (ii) normal-phase HPLC using a silica column (250 \times 10 mm; 5 μ m particles) with hexane/isopropanol (95:5 by vol) as the mobile phase. For both steps, UV absorbance at 212 nm was used for detection. The final isolate was confirmed as 7α -OOH by proton-NMR analysis (22) and quantified by iodometric analysis (23). Stock solutions in isopropanol were stable indefinitely when stored at $-20^\circ C$. $[^{14}C]7\alpha$ -OOH was prepared similarly, starting with $[4-^{14}C]$ Ch, the specific radioactivity of the isolated hydroperoxide typically being ~ 150 μ Ci/ μ mol.

Liposome preparation

Small unilamellar vesicles (SUV, 50 nm) of three different compositions were employed: DMPC/ 7α -OOH/Ch/DCP (49:25:25:1 by mol), POPC/ 7α -OOH/DCP (79:20:1 by mol), and POPC/DCP (99:1 by mol), stock preparations containing 5.0 mM total lipid in bulk suspension. The first type was used for 7α -OOH uptake and toxicity experiments, and the latter two for assessing binding of SCPI or 7α -OOH to recombinant SCP-2 in competition with NBD-Ch. For SUV preparation, lipid films were dried overnight in vacuo, vortex-suspended in Chlex-treated PBS (25 mM phosphate, 125 mM NaCl, pH 7.4), freeze-thawed 10 times, and extruded at room temperature using 0.05 μ m-pore polycarbonate membranes and an apparatus from Lipex Biomembranes (Vancouver, BC). The SUVs were stored under argon at

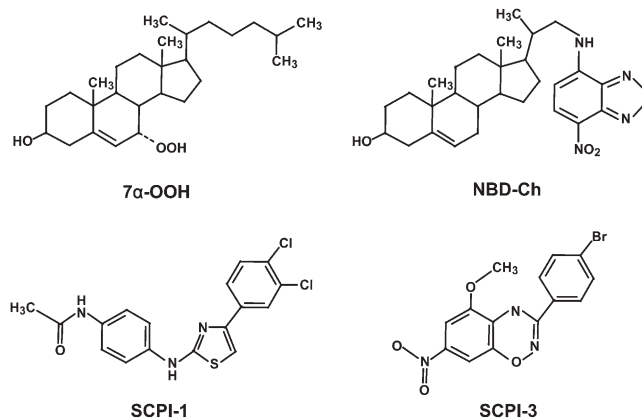


Fig. 1. Structures of 3β -hydroxycholesterol-5-ene- 7α -hydroperoxide (7α -OOH), 22-[*N*-(7-nitrobenz-2-oxa-1,3-diazol-4-yl)amino]23,24-bisnor-5-cholesterol-3 β -ol (NBD-Ch), *N*-(4-[[4-(3,4-dichlorophenyl)-1,3-thiazol-2-yl]amino]phenyl)acetamide (SCPI-1), and 3-(4-bromophenyl)-5-methoxy-7-nitro-4H-1,2,4-benzoxadiazine (SCPI-3).

4°C and used experimentally within 48 h. Other details were as described previously (15, 17).

Cell culture

An SCP-2-overexpressing transfectant clone (SC2F) of mouse L-cell fibroblasts (L arpt⁻ tk⁻), along with a vector control clone (VC), were kindly provided by Dr. Friedhelm Schroeder (Texas A&M University) as a gift. The cells were grown in DMEM containing 10% serum, penicillin (100 units/ml), streptomycin (0.1 mg/ml), and geneticin (G418, 0.35 mg/ml), using standard culture conditions. An SCP-2-overexpressing transfectant clone (SC2H) of rat McA-RH777 hepatoma cells, also obtained from Dr. Schroeder, was cultured under the same conditions (19). These cells had been transfected with a construct encoded for 15 kDa pro-SCP-2, which is posttranslationally converted to mature 13.2 kDa SCP-2 (7, 8). Human COH-BR1 cells, a breast cancer epithelial subline (24), were grown in DME-F12 medium supplemented as described above for DMEM. Transfectant cells were taken off selection agent (geneticin) at the second passage prior to an experiment.

Immunoblot analysis

The level of SCP-2 protein expressed in different cell lines was determined by Western blot analysis. Cells were recovered by trypsinization, washed with hypotonic buffer, and lysed by sonication. Lysates were centrifuged at 100,000 *g* for 1 h at 4°C. Proteins in supernatant fractions were separated by electrophoresis, using a 4–15% polyacrylamide gradient gel and transblotted to a 0.45 μ m polyvinylidene difluoride membrane. Blots were blocked, treated with rabbit anti-mouse SCP-2 (25), followed by peroxidase-conjugated anti-rabbit IgG, and then analyzed using enhanced chemiluminescence. Other details were as described previously (19).

Peroxide challenge in the absence vs. presence of SCP-2 inhibitors and evaluation of cell death

SCP-2-overexpressing SC2F and SC2H cells, along with vector controls, were grown to ~70% confluency in 12-well plates; COH-BR1 cells were prepared similarly. At 1 h before peroxide challenge, cells in serum-free medium at 37°C were treated with an SCP-2 inhibitor (SCPI-1 or SCPI-3) at various concentrations. The inhibitors were added from stock solutions in dimethylsulfoxide (DMSO), the final DMSO concentration in the medium being ~0.5% (v/v). Controls without the SCPIs contained the same concentration of DMSO. SCPI-1 and SCPI-3 were maintained at their initial levels throughout subsequent peroxide treatment. For the ChOOH challenge, cells were overlaid with 7 α -OOH-containing SUVs in DMEM, giving a range of initial hydroperoxide concentrations up to 200 μ M in bulk suspension. At 200 μ M 7 α -OOH, there was no significant cell detachment over at least a 6 h period. After a designated incubation time at 37°C (typically 4 h), the cells were washed free of SUVs, overlaid with 1% serum-containing DMEM, and after 20 h of additional incubation, checked for viability by thiazolyl blue (MTT) assay. Cells were treated with MTT (0.5 mg/ml in DMEM) for 4 h, then dissolved in isopropanol and the formazan level determined by measuring absorbance at 570 nm (26). SCPI-treated cells and their respective controls were also challenged with hydrogen peroxide (e.g., 1 mM H₂O₂ for 24 h), after which viability was checked by MTT assay.

To examine death mechanism, we incubated cells with a fixed concentration of liposomal 7 α -OOH (typically 175 μ M) for increasing time periods up to 6 h. After each period, the cells were treated with 5 μ M Ho and 50 μ M PI for 20 min at 37°C, then checked for extent of apoptosis versus necrosis by fluorescence microscopy, using a DAPI filter for Ho visualization and red filter

for PI. Ho detected sustained apoptosis, and PI confirmed any necrosis (27). For each sample, the number of stained nuclei in 4–5 viewing fields of ~100 cells each were determined.

Determination of 7 α -OOH uptake by cells in the absence versus presence of SCP-2 inhibitors

7 α -OOH uptake by SC2F cells and how this is affected by SCPI treatment was examined using a procedure similar to that described for studying hydroperoxide cytotoxicity, except for the use of radiolabeled 7 α -OOH in SUV donors, the stock DMPC/[¹⁴C]7 α -OOH/Ch/DCP (49:25:25:1 by mol) preparation containing 1.25 mM (~18 nCi/ml) hydroperoxide. Cells at ~70% confluency in 10 cm dishes were incubated with SCPI-1 or SCPI-3 for 1 h, followed by SUVs at a starting [¹⁴C]7 α -OOH concentration of ~100 μ M. At various times during incubation, the SUV-containing media were withdrawn, and cells were washed and recovered by scraping into PBS. After removing samples for protein determination, the cells were extracted with chloroform/methanol (2:1, v/v), as described (23). After centrifugation, an aliquot of lipid-containing lower phase was dried under argon, dissolved in 20 μ l of hexane/isopropanol (97:3 by vol), and analyzed for [¹⁴C]7 α -OOH by high performance thin layer chromatography with phosphorimaging detection (HPTLC-PI), using conditions described previously (28). HPTLC-PI is not only more sensitive than scintillation counting, but provides information about 7 α -OOH status (e.g., extent of any reduction to diol, 7 α -OH) (28). A known amount of starting SUVs was also analyzed by HPTLC-PI to establish specific analyte signal strength for the purpose of expressing uptake by cells on a molar basis.

Measurement of mitochondrial membrane potential ($\Delta\Psi_m$)

Cells in a 6-well plate were incubated with liposomal 7 α -OOH for 4.5 h in the absence or presence of a SCP-2 inhibitor, after which they were washed with PBS, overlaid with DMEM containing 2 μ M JC-1, a $\Delta\Psi_m$ probe (29), and then incubated for 30 min at 25°C. After washing again with PBS, the cells were recovered by gentle scraping, pelleted, resuspended in 2 ml of DMEM, and checked for fluorescence emission peaks in the red (550–610 nm) and green (490–550 nm) wavelength ranges, using 488 nm excitation and a Model QM-7SE spectrofluorimeter from Photon Technology International (London, Ontario, Canada). Peaks with maxima at 590 nm (red) and 530 nm (green) were integrated and their ratios calculated. A high red/green ratio reflects a strong $\Delta\Psi_m$, whereas a relatively low ratio reflects a weak $\Delta\Psi_m$ (29).

Measurement of cellular reactive oxidant level

The reactive oxygen species (ROS)-detecting probe, DCFH-DA, is taken up by cells and hydrolyzed to DCFH, which is trapped due to its greater polarity (30). DCFH in turn can be oxidized to DCF (the monitored fluorophore) by internally generated oxidants. At various time points during exposure to liposomal 7 α -OOH, cells were washed with PBS, incubated with DMEM containing 10 μ M DCFH-DA for 20 min at 37°C, washed again, overlaid with DMEM alone, and then examined by fluorescence microscopy using 488 nm excitation and 610 nm emission. The fluorescence intensity of representative image fields was determined using MetaMorphTM software.

SCPI and 7 α -OOH binding to SCP-2 assessed by competition with NBD-Ch

The ability of the SCPIs or 7 α -OOH to interact with isolated SCP-2 was examined by competitive binding assay, using NBD-Ch as the fluorescent substrate indicator. The general approach for measuring NBD-Ch binding was adapted from that described by

Colles et al. (12) and Avdulov et al. (31). For assessing SCPI binding, the reaction mixture (2.0 ml in a fluorescence cuvette) contained the following: 5 μM recombinant SCP-2, 1.25 μM NBD-Ch, and SCPI-1 or SCPI-3 in increasing concentrations from 0.2 to 10 μM in 10 mM phosphate/0.1 mM EDTA/0.1 mM DFO (pH 7.4). NBD-Ch and SCPI in dimethylformamide (DMF) were added together to the SCP-2, the final concentration of DMF being kept at 0.25 % (v/v) throughout. A reference mixture containing everything except SCPI was prepared alongside. After 5 min of incubation at 37°C with continuous stirring, emission spectra between 480 and 610 nm were recorded, using 460 nm excitation and band-pass slits of 5 nm and 7 nm for excitation and emission, respectively. Peaks were integrated and reductions in peak area caused by SCPI relative to a nonSCPI reference were calculated. A GraphPad Prism 4.0 program (GraphPad Software Inc., San Diego, CA) was used for data analysis [e.g., nonlinear regression curve fitting and determination of 50% binding inhibition (IC_{50}) parameters.]

For examining $7\alpha\text{-OOH}$ binding, liposomal $7\alpha\text{-OOH}$ in increasing concentrations from 0.5 to 25 μM was preincubated with 5 μM SCP-2 for 5 min in a fluorescence cuvette. POPC/ $7\alpha\text{-OOH}$ /DCP (79:20:1 by mol) SUVs were used. After addition of NBD-Ch (1.25 μM), reaction mixtures in 10 mM phosphate/0.1 mM EDTA/0.1 mM DFO (pH 7.4) were incubated again for 5 min at 37°C, after which emission spectra were recorded, as described above for SCPI binding. To account for any effects of liposomal lipid other than $7\alpha\text{-OOH}$, we recorded a similar set of spectra for reaction mixtures containing SCP-2, NBD-Ch, and levels of POPC/DCP (99:1 by mol) SUVs consistent with those for $7\alpha\text{-OOH}$ -containing SUVs. Spectra for mixtures lacking SCP-2 (0.5–25 μM liposomal $7\alpha\text{-OOH}$ plus 1.25 μM NBD-Ch) and for a mixture lacking liposomes (5 μM SCP-2 plus 1.25 μM NBD-Ch) were also recorded.

Possible interfering factors, such as interaction of NBD-Ch and SCP-2 with liposomes, were considered in carrying out these determinations. Binding of $7\alpha\text{-OOH}$ to SCP-2 in competition with NBD-Ch was evaluated by subtracting integrated peak areas for the SCP-2/NBD-Ch/ $7\alpha\text{-OOH}$ SUV system from those for the SCP-2/NBD-Ch/non- $7\alpha\text{-OOH}$ SUV system and plotting these differences as a function of $7\alpha\text{-OOH}$ concentration.

Statistics

The two-tailed Student's *t*-test was used for determining the significance of apparent differences between experimental values, with $P > 0.05$ considered statistically insignificant.

RESULTS

SCP-2 protein expression in the selected cell types

Three cell types producing relatively high levels of SCP-2 were used in this study, mouse fibroblast SC2F, rat hepatoma SC2H, and human COH-BR1, the first two representing SCP-2 transfectant clones and the third, wild-type cells. Western blot analysis revealed that the SC2F clone was substantially enriched in SCP-2 (Fig. 2A), β -actin-normalized densitometry indicating about a 3-fold elevation over the level in wild-type or VC cells. No significant difference in the level of other immunodetectable proteins, including SCP-x (7), was observed (not shown). SC2H cells exhibited about a 10-fold SCP-2 enrichment over their VC, and this level was ~ 5 times greater than that in SC2F cells (Fig. 2A). The constitutive level of SCP-2 in COH-BR1 cells was found to be ~ 9 times greater than that of L-cell VC (Fig. 2A) and also substantially greater than that of wild-type

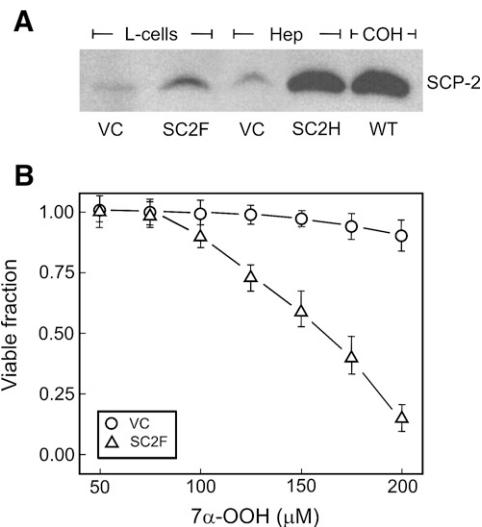


Fig. 2. SCP-2 protein expression in relation to $7\alpha\text{-OOH}$ cytotoxicity. A: Western blots of L-cell clones [vector control (VC) and SCP-2-transfectant (SC2F)], a hepatoma cell SCP-2-transfectant clone (SC2H), and wild-type COH-BR1 cells; protein loads: 50 μg per lane. Relative β -actin-normalized densitometry values are as follows: 1.0, 2.8, 7.1, and 9.3, respectively. B: Comparative sensitivities of clones VC and SC2F to $7\alpha\text{-OOH}$ -induced cell killing. SC2F (Δ) and VC (\circ) cells were incubated with $7\alpha\text{-OOH}$ -containing SUVs in increasing hydroperoxide concentration, as indicated, for 4 h and checked for viability by MTT assay 20 h later. Data points are means \pm SD of values from three replicated experiments.

hepatoma or L1210 leukemia cells (not shown). Why COH-BR1 cells naturally express SCP-2 in such relatively high amounts is not clear at present.

Toxic effects of $7\alpha\text{-OOH}$ on SC2F cells

SCP-2-overexpressing SC2F cells were found to be much more sensitive to liposomal $7\alpha\text{-OOH}$ -induced killing than VC as assessed by MTT assay (Fig. 2B), the LD_{50} values being ~ 0.16 mM and ~ 0.3 mM (estimated), respectively. Similar trends were observed previously for the hepatoma cells (i.e., $7\alpha\text{-OOH}$ was more toxic to transfectant clone SC2H than to its VC), but the LC_{50} levels in this case were lower, namely, ~ 19 μM and 75 μM , respectively (19). In contrast to $7\alpha\text{-OOH}$, H_2O_2 or *t*-butyl hydroperoxide was equally toxic to SC2F cells and their VC (results not shown), as was observed previously for SC2H cells and their VC (19). This suggests that specific binding/trafficking by SCP-2 occurred in the case of $7\alpha\text{-OOH}$ but H_2O_2 or *t*-butyl hydroperoxide, which lacks the structural characteristics of known SCP-2 ligands (7). We also found that there was no significant difference between SC2F and VC clones in the levels of antioxidant enzymes, such as catalase and glutathione peroxidase types 1 and 4, as well as total glutathione (results not shown). These findings rule out possible contributions of any of these factors to the observed differences in $7\alpha\text{-OOH}$ cytotoxicity (Fig. 2B).

Effects of SCP-2 inhibitors on $7\alpha\text{-OOH}$ and H_2O_2 toxicity toward SC2F cells

As shown in Fig. 3A, the SCP-2 inhibitor SCPI-1 in concentrations up to ~ 6 μM had no effect of the viability of

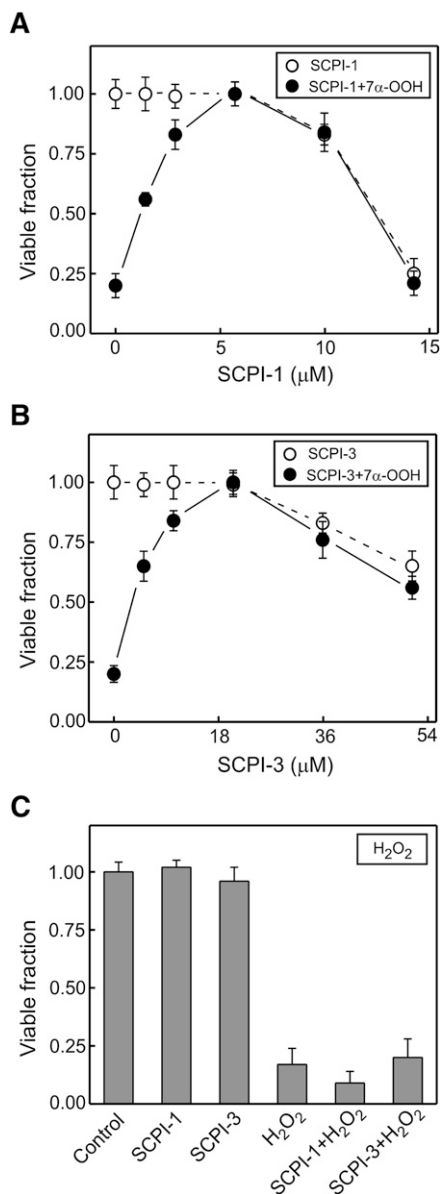


Fig. 3. Protective effects of SCP-2 inhibitors against hydroperoxide-induced SC2F cell killing. **A:** SCP-1: concentration-dependent toxicity (○) and protection against 7α-OOH toxicity (●). For assessing SCP-1 toxicity threshold, cells in serum-free DMEM were treated with inhibitor alone at the indicated concentrations for 5 h, then switched to 1% serum-containing DMEM, and MTT-based viability was determined 20 h later. For assessing cytoprotection, cells were preincubated with SCP-1 for 1 h, then exposed to 175 μM 7α-OOH in DMPC/7α-OOH/Ch/DCP (49:25:25:1 by mol) SUVs for 4 h, switched to 1% serum-containing DMEM, and checked for viability 20 h later; SCP-1 was maintained at the indicated concentrations throughout incubation with 7α-OOH. **B:** SCP-3: concentration-dependent toxicity (○) and protection against 7α-OOH toxicity (●). Other details were as described for SCP-1, except for the higher concentration range of SCP-3. **C:** H₂O₂: cells were preincubated with 6 μM SCP-1 or 21 μM SCP-3 for 1 h, then treated with 1.0 mM H₂O₂ for 24 h, after which viability was determined by MTT assay. SCP-1 or SCP-3 was present in the medium throughout the entire period of peroxide challenge in A, B, and C. Data points in each case are means ± SD of values from four separate experiments.

clone SC2F, but it exhibited a dose-dependent increase in cytotoxicity above this level. However, when added to cells prior to 7α-OOH, SCP-1 reduced peroxide-induced cell killing in a dose-dependent manner over the 0–6 μM range, 50% inhibition occurring at ~1.4 μM. Inhibitor SCP-3 was less toxic to SC2F cells, reducing viability only at concentrations above ~21 μM (Fig. 3B). When given to cells before 7α-OOH, SCP-3 protected against oxidative killing dose-dependently over the 0–21 μM range, 50% inhibition being seen at ~4.9 μM. Therefore, both SCPIs acted cytoprotectively in their nontoxic ranges, and SCP-1 was ~3.5 times more potent in this than SCP-3. A reasonable explanation is that the SCPIs interfered with cellular uptake/distribution of 7α-OOH by competing with it for binding to SCP-2. SCP-1 was not only more cytoprotective than SCP-3 at lower concentrations but also more cytotoxic on its own at higher concentrations, the LD₅₀ values above the toxic thresholds being ~13 μM and ~60 μM, respectively (Fig. 3A, B). In contrast to their strong anti-7α-OOH effects, neither SCP-1 nor SCP-3 at its most effective concentration with 7α-OOH provided any significant protection against cell killing by the nonlipid hydroperoxide H₂O₂ (Fig. 2C). This further supports our deduction from the observation that SC2F cells were no more sensitive to H₂O₂ than VC (see above), namely, that the 7α-OOH effects were dependent on interaction with SCP-2.

SCPI protective effects on other SCP-2-expressing mammalian cells

We tested the anti-7α-OOH effects of SCP-1 and SCP-3 on two other SCP-2-expressing cell types, hepatoma transfectant clone SC2H, shown previously to be hypersensitive to 7α-OOH toxicity (19), and COH-BR1 cells with high constitutive SCP-2 protein (Fig. 2). As shown in **Fig. 4A**, viability of SC2H cells was unaffected by 6 μM SCP-1 or 20 μM SCP-3. However, a liposomal 7α-OOH challenge under the conditions described reduced viability to ~12% of the control level after 20 h, and SCP-1 and SCP-3 at the indicated concentrations inhibited this nearly completely and by ~80%, respectively (Fig. 4A). In the case of COH-BR1 cells, SCP-1 and SCP-3 at the same concentrations used with SC2H cells were slightly toxic (10–20%) on their own, but once again, imposed a strong protection against 7α-OOH lethality (Fig. 4B). Thus, the observed SCPI protective effects appeared to be generally applicable to cells expressing significant levels of SCP-2. As in the case of SC2F cells (Fig. 2), both SCPIs became increasingly toxic to SC2H and more so to COH-BR1 cells (results not shown) at concentrations greater than those used in showing protection against 7α-OOH. This calls into question the assertion of Kim et al. (20) based on results with a single mammalian line, mouse breast cells, that SCPIs are minimally toxic to vertebrate cells.

SCPI inhibition of 7α-OOH uptake

A previous study (19) revealed that the initial rate of [¹⁴C]7α-OOH uptake by clone SC2H cells was significantly greater than that of a vector control, suggesting more rapid internalization of the peroxide due to binding by

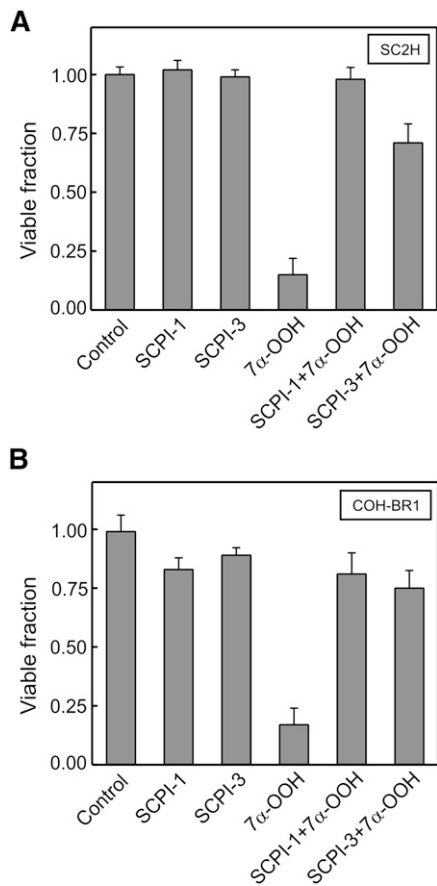


Fig. 4. SCPI protection of SC2H and COH-BR1 cells against 7 α -OOH-induced killing. A: Hepatoma clone SC2H cells in DMEM were incubated in the absence or presence of 6 μ M SCPI-1 or 21 μ M SCPI-3 for 1 h, then exposed to 75 μ M liposomal 7 α -OOH for 4 h, and checked for MTT-based viability after an additional 20 h. B: Breast tumor COH-BR1 cells in DME-F12 medium were incubated in the absence or presence of 6 μ M SCPI-1 or 21 μ M SCPI-3 for 1 h, then treated with 20 μ M liposomal 7 α -OOH for 4 h, and checked for viability 20 h later. In A and B, the SCPI were kept at the given concentrations throughout peroxide treatment; after 4 h with 7 α -OOH, cells were switched to 1% serum-containing medium. Plotted data are means \pm SD of values from four replicate experiments.

overexpressed SCP-2. Knowing this, we postulated that 7 α -OOH internalization would be slowed in SCPI-treated cells due to competitive interaction with SCP-2 and that this could at least partially explain the observed SCPI cytoprotective effects (Figs. 3 and 4). To study this, we examined the effects of SCPI preincubation on uptake of liposomal [14 C]7 α -OOH by SC2F cells. As shown by the HPTLC-PI profile in Fig. 5A, 7 α -OOH and its diol 7 α -OH could be detected in cells after a 1 h incubation with SUVs, the hydroperoxide band being less intense. Diol formation is attributed mainly to 7 α -OOH reduction in the cell compartment. The band intensity of both analytes was clearly reduced in samples from SCPI-treated cells (Fig. 5A). A plot of integrated band intensities (Fig. 5B) shows that cellular 7 α -OOH increased progressively with incubation time, reaching \sim 2 nmol/mg cell protein after 1 h and that SCPI-1 and SCPI-3 each lowered this by \sim 45%. Time-dependent accumulation of 7 α -OOH-derived 7 α -OH in cells

was likewise inhibited by the SCPIs (Fig. 5B). Thus, a reduced rate of 7 α -OOH uptake (along with intracellular distribution) is implicated in the SCPI cytoprotective effects seen in Figs. 3 and 4.

ROS accumulation in 7 α -OOH-treated cells: attenuation by SCPIs

ROS buildup in 7 α -OOH-treated SC2F cells was examined by fluorescence microscopy using DCFH-DA as a probe (30). Internalized DCFH-DA is trapped by being hydrolyzed to DCFH, which is converted to the fluorescent indicator DCF by strong oxidants (e.g., species generated by the action of endogenous peroxidases on H $_2$ O $_2$) (30). As shown in Fig. 6, DCF fluorescence intensity was very low initially but increased progressively with time of incubation with liposomal 7 α -OOH, reaching \sim 65 times the starting value by 6 h; at this point, \sim 50% of the cells were DCF-positive. No significant increase was observed for cells

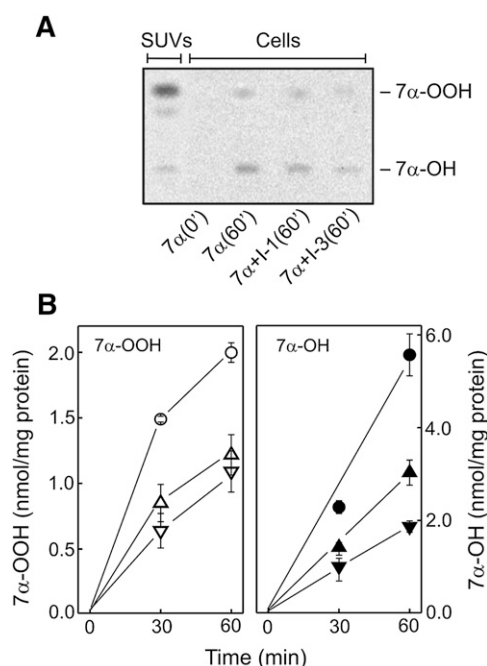


Fig. 5. SCPI interference with cellular uptake of 7 α -OOH. SC2F cells at a uniform confluence (\sim 70%) in 10 cm dishes were preincubated for 1 h in the absence or presence of 6 μ M SCPI-1 or 21 μ M SCPI-3, followed by 105 μ M (1.5 nCi/ml) [14 C]7 α -OOH in DMPC/[14 C]7 α -OOH/Ch/DCP (49:25:25:1 by mol) SUVs. After increasing times of incubation without or with either SCPI at the indicated concentration, SUV-containing media were removed, and the cells were washed once with cold PBS, then extracted with chloroform/methanol (2:1, v/v). Recovered lipid-containing fractions were analyzed by HPTLC-PI. A: Chromatographic profiles of cellular [14 C]7 α -OOH/7 α -OH immediately after SUV addition [7 (0')] and after a 60 min incubation period in the absence [7 (60')] or presence of SCPI-1 [7+I-1 (60')] or SCPI-3 [7+I-3 (60')]. Each lane corresponds to 42 μ g of cellular protein. Also represented is a lipid extract from the SUV donors containing 3.1 nmol of [14 C]7 α -OOH. B: Analyte accumulation in cells as a function of incubation time. Left panel: 7 α -OOH accumulation in the absence (○) or presence of SCPI-1 (△) or SCPI-3 (▽). right panel: 7 α -OH accumulation in the absence (●) or presence of SCPI-1 (▲) or SCPI-3 (▼). Means \pm deviation of values from duplicate experiments are shown.

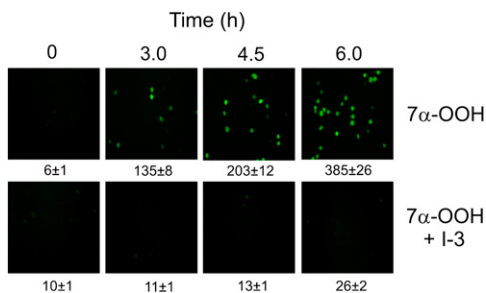


Fig. 6. SCPI inhibition of reactive oxidant accumulation in 7α -OOH-treated SC2F cells. Cells were incubated in the absence or presence of $21\ \mu\text{M}$ SCPI-3 for 1 h, after which $175\ \mu\text{M}$ liposomal 7α -OOH was introduced. At the indicated times after peroxide addition, the cells were treated with $10\ \mu\text{M}$ DCFH-DA for 20 min and then analyzed for DCF signals by fluorescence microscopy. Integrated intensity level is indicated below each viewing field; means \pm SD of values from three separate experiments are shown. 7α -OOH, 3β -hydroxycholest-5-ene- 7α -hydroperoxide; DCFH-DA, 2',7'-dichlorofluorescein diacetate; DCF, 2',7'-dichlorofluorescein; SCPI-3, 3-(4-bromophenyl)-5-methoxy-7-nitro-4H-1,2,4-benzoxadiazine.

treated with SUVs lacking 7α -OOH or containing 7α -OH instead (not shown). In striking contrast to the results with 7α -OOH alone, cells treated with $20\ \mu\text{M}$ SCPI-3 before the hydroperoxide showed relatively little DCF fluorescence throughout, the intensity at 6 h being only ~ 3 times greater than that at the outset (Fig. 6). A dramatic reduction in DCF signal intensity was also observed when cells were preincubated with SCPI-1 (not shown). Thus, there was a strong correlation between the SCPI effects on ROS accumulation and cell killing (Figs. 3 and 4). Based on previous evidence (19), it is likely that most of these oxidants were secondary species arising from one-electron turnover of incoming 7α -OOH, most of the latter having already reacted before DCFH-DA was introduced.

SCPI inhibition of $\Delta\Psi_m$ loss and apoptotic cell death provoked by 7α -OOH

Exposure of SC2F cells to 7α -OOH resulted in a loss of mitochondrial membrane potential, as measured by JC-1 red/green emission ratio, the value after 4 h of continuous incubation being $\sim 15\%$ of the control without 7α -OOH (Fig. 7). The mitochondrial uncoupling agent valinomycin produced a similar large loss of $\Delta\Psi_m$. In cells treated with the SCPIs prior to 7α -OOH, $\Delta\Psi_m$ loss was much less, $6\ \mu\text{M}$ SCPI-1 attenuating it by $\sim 42\%$ and $20\ \mu\text{M}$ SCPI-3 by $\sim 35\%$ (Fig. 7). The ability of these SCPIs to at least partially preserve $\Delta\Psi_m$ under 7α -OOH pressure is consistent with their observed cytoprotective effects (Figs. 3 and 4).

The mechanism of SC2F cell death induced by 7α -OOH was examined by fluorescence imaging using the nuclear dyes Ho and PI. As shown in Fig. 7A, cells treated for up to 6 h with $0.175\ \text{mM}$ liposomal 7α -OOH died mainly by apoptosis rather than necrosis (i.e., the number of cells with Ho-positive nuclei increased progressively throughout while those with PI-positive nuclei remained insignificant). Apoptosis was negligible (less than 5% of cells) at time-zero or in controls incubated with SUVs lacking 7α -OOH

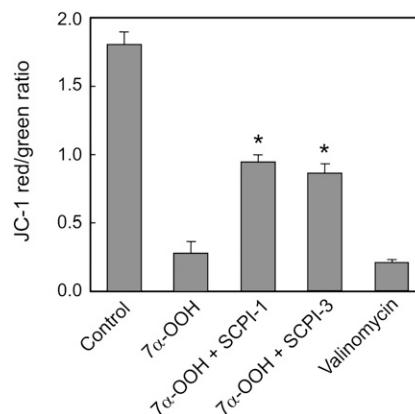


Fig. 7. SCPI protection against peroxide-induced loss of mitochondrial membrane potential. SC2F cells were incubated in the absence or presence of $6\ \mu\text{M}$ SCPI-1 or $21\ \mu\text{M}$ SCPI-3 for 1 h and then in the presence of $175\ \mu\text{M}$ SUV- 7α -OOH for 4 h. After removal of the SUV-containing medium, cells were overlaid with fresh medium containing $2\ \mu\text{M}$ JC-1 and 30 min later were recovered for measurement of JC-1 red and green fluorescence spectra. Peaks with maxima at $590\ \text{nm}$ (red) and $530\ \text{nm}$ (green) were integrated and their ratios calculated as indices of $\Delta\Psi_m$ status. Also represented are cells treated with JC-1 after being exposed to $1\ \mu\text{M}$ valinomycin for 30 min. Plotted values are means \pm SD ($n = 4$).

(not shown). When cells were preincubated with $6\ \mu\text{M}$ SCPI-1 or $20\ \mu\text{M}$ SCPI-3, the extent of apoptosis under 7α -OOH challenge was dramatically reduced (Fig. 8A). Plotted data from these experiments (Fig. 8B) indicate that apoptotic cell count under peroxide exposure increased steadily to $\sim 60\%$ after 6 h. Each of the SCPIs reduced the apoptotic count by at least 90%.

SCPI and 7α -OOH binding to isolated SCP-2

Direct competition between the SCPIs and 7α -OOH for binding to SCP-2 could explain the observed abilities of the former to inhibit cell uptake and cytotoxic effects of the latter, including damaging ROS production, loss of $\Delta\Psi_m$, and apoptotic cell killing. Relatively simple cell-free systems involving human recombinant SCP-2, NBD-Ch, 7α -OOH, and the SCPIs were set up to begin investigating this question. Using NBD-Ch as a reporter with greatly increased fluorescence quantum yield upon interaction with SCP-2 (12, 31), we studied two basic binding models: one involving competition between SCPI-1 or SCPI-3 and NBD-Ch for SCP-2, and the other competition between 7α -OOH and NBD-Ch for SCP-2. As shown in Fig. 9A, fluorescence of NBD-Ch was greatly enhanced upon interaction with SCP-2, the integrated peak area of NBD-Ch + SCP-2 [trace (a)] being ~ 30 times greater than that of NBD-Ch alone [trace (g)]. When included in the reaction mixture, SCPI-1 reduced the NBD fluorescence in a concentration-dependent manner over the 0.25 – $10\ \mu\text{M}$ range [Fig. 9A, traces (b)–(f)]; SCPI-3 also reduced the NBD signal, albeit less potently (not shown). For each inhibitor, percent reduction of integrated fluorescence peak intensity was plotted as a function of concentration (Fig. 9B). As can be seen, both inhibitors competed with NBD-Ch, exhibiting an approach to saturation with increasing concentration, SCPI-1

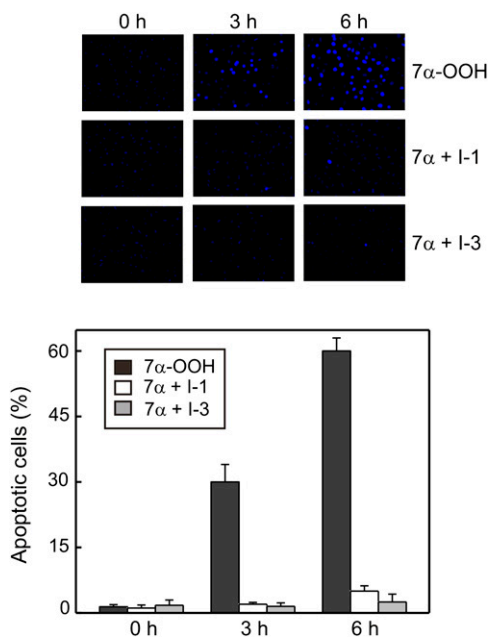


Fig. 8. SCPI inhibition of 7α -OOH-provoked apoptotic cell death. SC2F cells were incubated in the absence or presence of SCPI-1 (6 μ M) or SCPI-3 (21 μ M) for 1 h, then exposed to 175 μ M SUV- 7α -OOH for the indicated times at 37°C. Immediately thereafter, the SUV-containing media were removed, and after washing with PBS, the cells were treated with Ho and PI and examined for apoptotic (blue-staining) versus necrotic (red-staining) nuclei by fluorescence microscopy. Representative images for each experimental condition are shown. Plotted data show percent apoptotic cells as a function of incubation time with SUV- 7α -OOH in the absence or presence of SCPI-1 or SCPI-3. Means \pm SD of values from four independent experiments are shown.

competing more effectively than SCPI-3. Using a software program for extracting competitive binding parameters, we determined that the IC_{50} values for SCPI-1 and SCPI-3 were 3.32 μ M and 6.50 μ M, respectively.

The situation was more complicated in the case of 7α -OOH. For some unknown reason, adding DMF solutions of 7α -OOH plus NBD-Ch to SCP-2 did not give consistent competitive binding results as had been observed for DMF solutions of the SCPIs plus NBD-Ch. Switching to ethanol as a vehicle did not improve the situation. However, when 7α -OOH was presented in liposomal (SUV) form, as used with cells, highly reproducible, concentration-dependent results were obtained, showing that the hydroperoxide competes with NBD-Ch for binding to SCP-2. Nevertheless, the analysis was more complicated because enhanced fluorescence due to NBD-Ch interaction with the SUVs had to be corrected for. **Fig. 10A** shows emission spectra for NBD-Ch at a single concentration in the presence of no additions [trace (a)], 7α -OOH-containing SUVs alone [trace (b)], SCP-2 alone [trace (c)], 7α -OOH-containing SUVs plus SCP-2 [trace (d)], or POPC-only SUVs plus SCP-2 [trace (e)]. The integrated area under trace (d) was found to equal that under trace (b) plus trace (c), indicating that the SCP-2 and SUV effects on NBD-Ch fluorescence were additive. As shown in Fig. 10A, the trace (d) signal was lower than that of trace (e), suggesting that

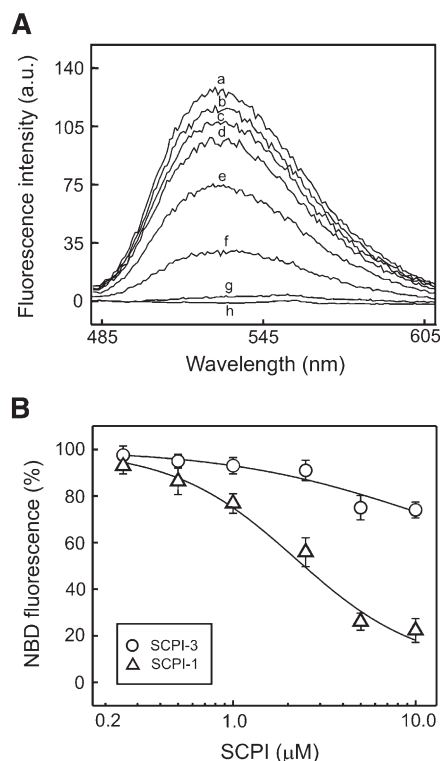


Fig. 9. Competition between SCPI and NBD-Ch for binding to isolated SCP-2. **A:** Fluorescence emission spectra of 1.25 μ M NBD-Ch in the presence of 5 μ M recombinant SCP-2 and SCPI-1 in increasing concentrations from 0 μ M to 10 μ M [traces (a)-(f)]. Traces (g) and (h) represent NBD-Ch alone and SCP-2 alone, respectively. All final reaction mixtures contained 0.25% (v/v) dimethylformamide, the solvent used for NBD-Ch and the SCPIs. **B:** Fluorescence peaks from A and from a similar experiment using 0–10 μ M SCPI-3 were integrated, and the level of NBD-Ch fluorescence relative to that in the absence of SCPI was plotted against SCPI concentration. Values are means \pm SD ($n = 4$).

NBD-Ch binding by SCP-2 was diminished by 7α -OOH. A single concentration of SUV 7α -OOH (10 μ M) is represented in Fig. 10A. Fig. 10B shows a plot of peak area as a function of 7α -OOH concentration for the NBD-Ch/SCP-2/ 7α -OOH SUV system and as a function of corresponding total lipid concentration for the NBD-Ch/SCP-2/all-POPC SUV system. Note that the concentration-dependent increase in peak area was much lower for the 7α -OOH-containing system. Fig. 10C shows a plot of percent reduction of fluorescence signal by 7α -OOH relative to the signal with total lipid over the given concentration range. This represents the corrected titration curve for competitive 7α -OOH binding to SCP-2. Data analysis by the same approach described for Fig. 9B revealed that the IC_{50} for 7α -OOH was 12.6 μ M. Thus, the avidity of 7α -OOH for SCP-2 appeared to be $\sim 1/4$ that of SCPI-1 and $1/2$ that of SCPI-3.

DISCUSSION

Oxidative stress-generated hydroperoxides (including H_2O_2 arising from upstream reactions, such as $O_2^{\cdot-}$ reduction/dismutation, and LOOHs generated secondarily

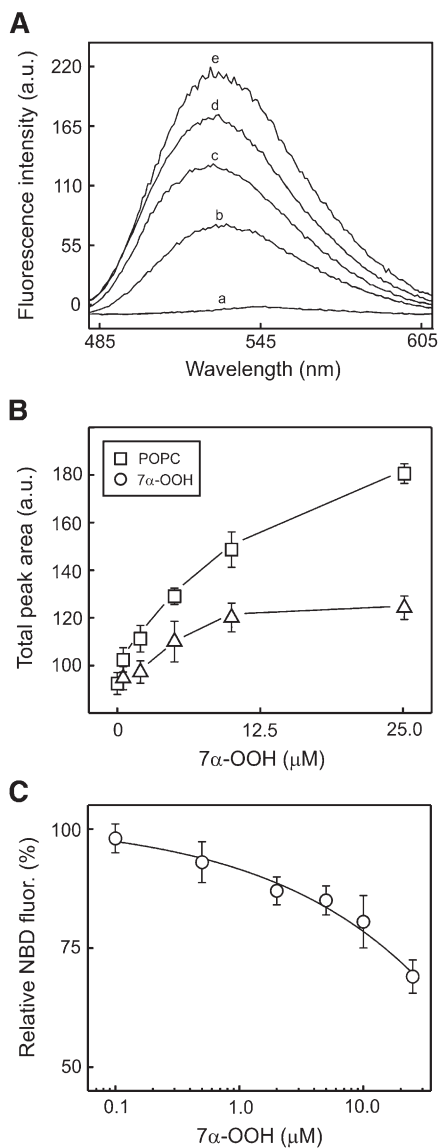


Fig. 10. Competition between SCPI and liposomal 7 α -OOH for binding to isolated SCP-2. A: Fluorescence emission spectra of 1.25 μ M NBD-Ch in the presence of the following other components: (a) none; (b) 10 μ M 7 α -OOH in POPC/7 α -OOH/DCP (79:20:1 by mol) SUV form; (c) 5 μ M SCP-2; (d) 5 μ M SCP-2 plus 10 μ M 7 α -OOH in SUV form; (e) 5 μ M SCP-2 plus 10 μ M POPC in POPC/DCP (99:1 by mol) form. NBD-Ch (1.25 μ M) plus 10 μ M POPC in SUV form gave a spectrum (not shown) that was virtually identical to that of (b). B: Fluorescence peak areas for conditions (d) and (e) in panel A plotted as a function of 7 α -OOH concentration over the 0.5–25 μ M range (Δ). The POPC plot (\square) represents total lipid concentrations for the given range of peroxide concentrations; for example, at 10 μ M 7 α -OOH, total lipid was 50 μ M, as 7 α -OOH was 20 mol % of the SUV lipid. C: Replotted panel B data showing NBD-Ch fluorescence in the presence of SUV-7 α -OOH relative to that in the presence of total SUV lipid, as a function of 7 α -OOH concentration. Values in B and C are means \pm SD ($n = 3$).

via attack of ROS, such as $^1\text{O}_2$ or H_2O_2 -derived $\text{HO}\cdot$ on cell membrane lipids) are well known for their nonspecific cytotoxic effects, although in low doses these species may also play a more subtle and selective role as redox signaling molecules (32–34). Being relatively small and hydro-

philic, H_2O_2 may readily translocate from its site of origin/entry in a cell, and depending on access to detoxifying enzymes, this could be a crucial factor in its cytotoxic/signaling activity. These effects of H_2O_2 have been widely studied, but little is known about its subcellular movement or distribution under stress conditions. This also applies to the more complex LOOHs. However, recent recognition that LOOH activity is not necessarily restricted to a membrane of origin in a cell but may be “broadcasted” elsewhere by spontaneous or protein-mediated translocation (15–18) has opened up a new area of investigation in the oxidative stress field. The first studies to demonstrate that LOOH redox toxicity can be disseminated via intermembrane transfer were carried out in this laboratory using 7 α -OOH and other ChOOH isomers (15, 17). Using membrane donor-acceptor model systems, we found that the ChOOHs spontaneously translocated at different rates but much faster than unoxidized Ch, consistent with more rapid departure due to greater hydrophilicity (17). For example, 7 α -OOH moved with a first-order rate constant that was ~ 200 times that of Ch (17). Subsequent studies showed that ChOOH transfer could be further enhanced by naturally occurring or recombinant SCP-2, the first known evidence for LOOH translocation by a cellular lipid-trafficking protein (18). When isolated liver mitochondria were used as acceptors, transfer uptake of 7 α -OOH from SUV donors was accelerated by recombinant SCP-2, resulting in a more rapid loss of membrane potential due to damaging free-radical reactions induced by iron-catalyzed reduction of the hydroperoxide (18). Similar results were reported recently for recombinant StarD4 (35), a sterol-specific transfer protein that delivers Ch to mitochondria of steroidogenic cells for the initial stages of steroid hormone biosynthesis (4, 5).


Of greater relevance to the present study is earlier work (19) involving SCP-2-overexpressing rat hepatoma cells, which we now refer to as clone SC2H. We showed that these cells, expressing ~ 10 times more immunodetectable SCP-2 than vector controls, were substantially more sensitive to 7 α -OOH lethality than the controls but equally sensitive to H_2O_2 - or *t*-butyl hydroperoxide lethality, consistent with the former being SCP-2-mediated. Moreover, [^{14}C]7 α -OOH was internalized faster by SC2H cells (presumably via interaction with SCP-2) and accumulated faster in mitochondria than in other subcellular compartments (19). Tracking experiments showed that [^{14}C]7 α -OOH underwent more extensive one-electron (toxic) turnover in SC2H cells than controls, as well as greater time-dependent ROS buildup, loss of mitochondrial membrane potential, and lipid peroxidation in situ, localized mainly to mitochondria (19). These results were consistent with SCP-2-dependent trafficking and mitochondrial targeting of 7 α -OOH, although direct evidence for SCP-2 interaction with the hydroperoxide was lacking. This issue was addressed in the present study through the use of selected SCP-2 inhibitors (i.e., agents shown previously to interfere with Ch binding by mosquito SCP-2) (20, 21). The initial purpose of those studies (20) was to discover potential pharmacologic inhibitors of yellow fever mosquito SCP-2,

which, through Ch trafficking, plays an essential role in insect survival and development. High-throughput screening of a small molecule chemical library identified a group of compounds that not only competed with NBD-Ch for binding to mosquito recombinant SCP-2 but also reduced Ch uptake by insect cells, acted as potent larvicides, and had minimal toxicity toward mammalian cells (20). We have shown that two of these compounds, SCPI-1 and SCPI-3 in sub-toxic concentrations, strongly inhibit 7α -OOH uptake by SCP-2-overexpressing SC2F cells while protecting them against lethal oxidative damage manifested by $\Delta\Psi_m$ loss and apoptotic death. Importantly, SC2F cell killing by a nonlipid hydroperoxide, H_2O_2 , was not affected by either of these inhibitors (Fig. 3C), suggesting that SCP-2 was not involved in this case. In agreement, there is no known evidence that SCP-2 can bind/translocate H_2O_2 . However, if the latter gave rise to any ChOOH in our cellular system (e.g., via Fenton chemistry), this appeared to be inconsequential. The noninvolvement of SC2F cell SCP-2 in H_2O_2 toxicity agrees with our earlier observation that H_2O_2 was no more toxic to SC2H cells than to the vector control or wild-type counterparts (19). SCPI-inhibitable 7α -OOH toxicity, which was demonstrated in two other high SCP-2-expressing cell types, transfectant clone SC2H and wild-type COH-BR1, strengthens our argument that the transfer protein played a direct role in the lethal effects.

Further support for this argument was obtained by examining the ability of SCPIs or 7α -OOH to interfere with NBD-Ch binding by recombinant human SCP-2. Fluorometric measurements of this binding were modeled after those first carried out by Colles et al. (12). Using these cell-free conditions, we showed that SCPI-1 and SCPI-3 both competed with NBD-Ch for binding, the latter $\sim 50\%$ less effectively than the former. These findings are qualitatively similar to those reported previously for interaction of these SCPIs with mosquito SCP-2 (20, 21). In parallel experiments, we demonstrated that 7α -OOH also competed with NBD-Ch for SCP-2 binding, although more weakly than the SCPIs. The implication of these findings collectively is that 7α -OOH associates with SCP-2 in a manner similar to Ch and that SCPI-1 or SCPI-3 can block this. In accordance, 7α -OOH retains general structural features of Ch, with polar groups in the A/B-ring "head" region and the same hydrophobic "tail" region (Fig. 1). Based largely on these observations with isolated SCP-2, we assert that binding and transport by cellular SCP-2 played a key role in 7α -OOH cytotoxicity and that competitive binding by the SCPIs explains their protective effects (Figs. 3 and 4). It is important to point out that the SPCI results suggest that any nonspecific effects of SCP-2 overexpression, such as changes in membrane lipid composition, (36) appear to have been relatively unimportant as determinants of elevated 7α -OOH toxicity.

The SCPIs used in this study were discovered by Kim et al. (20) in terms of their ability to inhibit vital SCP-2-mediated Ch transport and metabolism in mosquitoes. Our finding that these SCPIs interfere with NBD-Ch and 7α -OOH binding by a mammalian SCP-2 suggests that the

insect and mammalian proteins interact similarly with the SCPIs and with natural ligands like Ch. In support of this, recent studies have shown a remarkable degree of tertiary structural similarity between mammalian and insect SCP-2 despite only $\sim 30\%$ sequence identity (37, 38). Although a high-resolution structure for any Ch-bound SCP-2 is yet to be elucidated, it is likely that a large hydrophobic cavity known to exist in both the insect and mammalian proteins (8, 37, 38) will be occupied by the sterol, and similar binding is predicted for 7α -OOH.

In summary, we have shown that intracellular SCP-2, which normally translocates Ch for membrane homeostasis and other metabolic purposes, can also bind and transfer 7α -OOH, a free radical-generated hydroperoxide of Ch, and that this puts cells at greater risk of lethal oxidative injury. These findings provide further support for the hypothesis that under oxidative-stress conditions, inappropriate SCP-2 trafficking of 7α -OOH and other LOOHs will greatly expand their damaging and signaling ranges, thus exacerbating the stress response. A plausible explanation for these effects is that toxic hydroperoxide turnover or induction of death signaling at subcellular delivery sites exceeds the capacity for detoxification at these sites (16). We challenged cells with 7α -OOH from an exogenous source (SUVs), which could model transfer uptake occurring in the circulation (e.g., from peroxidized low density lipoprotein) (39). In mammalian cells under an endogenous oxidative challenge, the plasma membrane would serve as the richest transfer donor of 7α -OOH and other ChOOHs, because most of the cellular Ch (over 80%) typically resides in this compartment (40). We showed previously (18) that isolated recombinant SCP-2 can accelerate intermembrane transfer of phospholipid hydroperoxides in addition to ChOOHs, consistent with its known low selectivity for lipid ligands (7, 8). Thus, we anticipate that cellular SCP-2 would also amplify phospholipid hydroperoxide cytotoxicity, but this remains to be investigated. Our recent studies have shown that another intracellular lipid transfer protein, StarD4, can also transport 7α -OOH and Ch (35). In this case, however, absolute specificity for the sterol nucleus was demonstrated, phospholipid hydroperoxides (like parent phospholipids) not being recognized by the protein (35). It remains to be determined whether intracellular transfer proteins with a known high specificity for phospholipids (9) will enhance oxidative toxicity and/or signaling by selectively trafficking phospholipid-derived hydroperoxides. 

The authors are grateful to Dr. Friedhelm Schroeder for kindly supplying us with the SCP-2-overexpressing clones or L-cells and hepatoma cells, along with their vector controls. Helpful advice from the Schroeder laboratory regarding the maintenance of these cells in culture and evaluation of SCP-2 expression is also appreciated.

REFERENCES

1. Phillips, M. C., W. J. Johnson, and G. H. Rothblat. 1987. Mechanisms and consequences of cellular cholesterol exchange and transfer. *Biochim. Biophys. Acta.* **906**: 223–276.

2. Dawidowicz, E. A. 1987. Lipid exchange: transmembrane movement, spontaneous movement, and protein-mediated transfer of lipids and cholesterol. *In* Current Topics in Membranes and Transport. Vol. 29. R.D. Klausner, C. Kempf, and J. van Renswoude, editors. Academic Press, New York. 175–202.
3. Brown, R. E. 1992. Spontaneous lipid transfer between organized lipid assemblies. *Biochim. Biophys. Acta.* **1113**: 375–389.
4. Soccio, R. E., and J. L. Breslow. 2003. StAR-related lipid transfer (START) proteins: mediators of intracellular lipid metabolism. *J. Biol. Chem.* **278**: 22183–22186.
5. Miller, W. L. 2007. Steroidogenic acute regulatory protein (StAR), a novel mitochondrial cholesterol transporter. *Biochim. Biophys. Acta.* **1771**: 663–676.
6. Scallen, T. J., A. Pastuszyn, B. J. Noland, R. Chanderbhan, A. Kharroubi, and G. V. Vanhouny. 1985. Sterol carrier and lipid transfer proteins. *Chem. Phys. Lipids.* **38**: 239–261.
7. Gallegos, A. M., B. P. Atshaves, S. M. Storey, O. Starodub, A. D. Petrescu, H. Huang, A. L. McIntosh, G. G. Martin, H. Chao, A. B. Kier, et al. 2001. Gene structure, intracellular localization, and functional roles of sterol carrier protein-2. *Prog. Lipid Res.* **40**: 498–563.
8. Stollowich, N. J., A. D. Petrescu, H. Huang, G. G. Martin, A. I. Scott, and F. Schroeder. 2002. Sterol carrier protein-2: structure reveals function. *Cell. Mol. Life Sci.* **59**: 193–212.
9. Wirtz, K. W. A. 2006. Phospholipid transfer proteins in perspective. *FEBS Lett.* **580**: 5436–5441.
10. Starodub, O., C. A. Jolly, B. P. Atshaves, J. B. Roths, E. J. Murphy, A. B. Kier, and F. Schroeder. 2000. Sterol carrier protein-2 immunolocalization in endoplasmic reticulum and stimulation of phospholipid formation. *Am. J. Physiol. Cell Physiol.* **279**: C1259–C1269.
11. Woodford, J. K., S. M. Colles, S. C. Myers-Payne, J. T. Billheimer, and F. Schroeder. 1995. Sterol carrier protein-2 stimulates intermembrane sterol transfer by direct membrane interaction. *Chem. Phys. Lipids.* **76**: 73–84.
12. Colles, S. M., J. K. Woodford, D. Moncecchi, S. C. Myers-Payne, L. R. McLean, J. T. Billheimer, and F. Schroeder. 1995. Cholesterol interaction with recombinant human sterol carrier protein-2. *Lipids.* **30**: 795–803.
13. Porter, N. A., S. E. Caldwell, and K. A. Mills. 1995. Mechanisms of free radical oxidation of unsaturated lipids. *Lipids.* **30**: 277–290.
14. Girotti, A. W. 1998. Lipid hydroperoxide generation, turnover, and effector action in biological systems. *J. Lipid Res.* **39**: 1529–1542.
15. Vila, A., W. Korytowski, and A. W. Girotti. 2000. Dissemination of peroxidative stress via intermembrane transfer of lipid hydroperoxides: model studies with cholesterol hydroperoxides. *Arch. Biochem. Biophys.* **380**: 208–218.
16. Girotti, A. W. 2008. Translocation as a means of disseminating lipid hydroperoxide-induced oxidative damage and effector action. *Free Radic. Biol. Med.* **44**: 956–968.
17. Vila, A., W. Korytowski, and A. W. Girotti. 2001. Spontaneous intermembrane transfer of various cholesterol-derived hydroperoxide species: kinetic studies with model membranes and cells. *Biochemistry.* **40**: 14715–14726.
18. Vila, A., V. V. Levchenko, W. Korytowski, and A. W. Girotti. 2004. Sterol carrier protein-2-facilitated intermembrane transfer of cholesterol- and phospholipid-derived hydroperoxides. *Biochemistry.* **43**: 12592–12605.
19. Kriska, T., V. V. Levchenko, W. Korytowski, B. P. Atshaves, F. Schroeder, and A. W. Girotti. 2006. Intracellular dissemination of peroxidative stress: internalization, transport, and lethal targeting of a cholesterol hydroperoxide species by sterol carrier protein-2-overexpressing hepatoma cells. *J. Biol. Chem.* **281**: 23643–23651.
20. Kim, M. S., V. Wessely, and Q. Lan. 2005. Identification of mosquito sterol carrier protein-2 inhibitors. *J. Lipid Res.* **46**: 650–657.
21. Larson, R. T., V. Wessely, Z. Jiang, and Q. Lan. 2008. Larvicidal activity of a sterol carrier protein-2 inhibitor in four species of mosquitoes. *J. Med. Entomol.* **45**: 439–444.
22. Korytowski, W., P. G. Geiger, and A. W. Girotti. 1999. Lipid hydroperoxide analysis by high-performance liquid chromatography with mercury cathode electrochemical detection. *Methods Enzymol.* **300**: 23–33.
23. Girotti, A. W., and W. Korytowski. 2000. Cholesterol as a singlet oxygen detector in biological systems. *Methods Enzymol.* **319**: 85–100.
24. Esworthy, R. S., M. A. Baker, and F-F. Chu. 1995. Expression of selenium-dependent glutathione peroxidase in human breast tumor lines. *Cancer Res.* **55**: 957–962.
25. Atshaves, B. P., A. D. Petrescu, O. Starodub, J. B. Roths, A. B. Kier, and F. Schroeder. 1999. Expression and intracellular processing of the 58 kDa sterol carrier protein-2/3-oxoacyl-CoA thiolase in transfected mouse L-cell fibroblasts. *J. Lipid Res.* **40**: 610–622.
26. Mossman, T. 1983. Rapid colorimetric assay for cellular growth and survival: application to proliferation and cytotoxicity assays. *J. Immunol. Methods.* **65**: 55–63.
27. Spector, D. L., R. D. Goldman, and L. A. Leinwald, editors. 1997. Cells: a Laboratory Manual. Vol. 1. Cold Spring Harbor Laboratory Press, New York.
28. Korytowski, W., M. Wrona, and A. W. Girotti. 1999. Radiolabeled cholesterol as a reporter for assessing one-electron turnover of lipid hydroperoxides. *Anal. Biochem.* **270**: 123–132.
29. Reers, M., S. T. Smiley, C. Mottola-Hartshorn, A. Chen, M. Lin, and L. B. Chen. 1995. Mitochondrial membrane potential monitored by JC-1 dye. *Methods Enzymol.* **260**: 406–417.
30. LeBel, C. P., H. Ischiropoulos, and S. C. Bondy. 1992. Evaluation of the probe 2',7'-dichlorofluorescein as an indicator of reactive oxygen species formation and oxidative stress. *Chem. Res. Toxicol.* **5**: 227–231.
31. Avdulov, N. A., S. V. Chochina, U. Igbavboa, C. S. Warden, F. Schroeder, and W. G. Wood. 1999. Lipid binding to sterol carrier protein-2 is inhibited by ethanol. *Biochim. Biophys. Acta.* **1437**: 37–45.
32. Veal, E. A., A. M. Day, and B. A. Morgan. 2007. Hydrogen peroxide sensing and signaling. *Mol. Cell.* **26**: 1–14.
33. D'Autreaux, B., and M. B. Toledano. 2007. ROS as signalling molecules: mechanisms that generate specificity in ROS homeostasis. *Mol. Cell. Biol.* **8**: 813–824.
34. Forman, H. J., M. Maiorino, and F. Ursini. 2010. Signaling functions of reactive oxygen species. *Biochemistry.* **49**: 835–842.
35. Korytowski, W., D. Rodriguez-Agudo, A. Pilat, and A. W. Girotti. 2010. StarD4-mediated translocation of 7-hydroperoxycholesterol to isolated mitochondria: deleterious effects and implications for steroidogenesis under oxidative stress conditions. *Biochem. Biophys. Res. Commun.* **392**: 58–62.
36. Murphy, E. J., T. Stiles, and F. Schroeder. 2000. Sterol carrier protein-2 expression alters phospholipid content and fatty acyl composition in L-cell fibroblasts. *J. Lipid Res.* **41**: 788–796.
37. Choinowski, T., H. Hauser, and K. Piontek. 2000. Structure of sterol carrier protein-2 at 1.8 Å resolution reveals a hydrophobic tunnel suitable for lipid binding. *Biochemistry.* **39**: 1897–1902.
38. Dyer, D. H., S. Lovell, J. B. Thoden, H. M. Holden, I. Rayment, and Q. Lan. 2003. The structural determination of an insect sterol carrier protein-2 with a ligand-bound C16 fatty acid at 1.35 Å resolution. *J. Biol. Chem.* **278**: 39085–39091.
39. Vila, A., W. Korytowski, and A. W. Girotti. 2002. Spontaneous transfer of phospholipid and cholesterol hydroperoxides between cell membranes and low density lipoprotein: assessment of reaction kinetics and prooxidant effects. *Biochemistry.* **41**: 13705–13716.
40. Bloch, K. E. 1983. Sterol structure and membrane function. *Crit. Rev. Biochem.* **14**: 47–92.